2016

Depth Profiles of Persistent Organic Pollutants in the North and Tropical Atlantic Ocean

Caoxin Sun

Thomas Soltwedel

See next page for additional authors

Citation/Publisher Attribution
Sun, C., Soltwedel, T., Bauerfeind, E., Adelman, D. A., & Lohmann, R. (2016). Depth Profiles of Persistent Organic Pollutants in the North and Tropical Atlantic Ocean. *Environ. Sci., Technol., 50*(12): 6172-6179.
Available at: http://dx.doi.org/10.1021/acs.est.5b05891

Depth profiles of persistent organic pollutants in the North and Tropical Atlantic Ocean

*Caoxin Sun[1], Thomas Soltwedel[2], Eduard Bauerfeind,[2] Dave A. Adelman[1], Rainer Lohmann[1,]**

[1]Graduate School of Oceanography, University of Rhode Island, South Ferry Road, Narragansett, 02882 Rhode Island, United States

[2]Alfred-Wegener-Institut, Helmholtz-Zentrum für Polar- und Meeresforschung, Am Handelshafen 12, 27570 Bremerhaven, Germany

ABSTRACT

Little is known of the distribution of persistent organic pollutants (POPs) in the deep ocean. Polyethylene passive samplers were used to detect the vertical distribution of truly dissolved POPs at two sites in the Atlantic Ocean. Samplers were deployed at five depths covering 26-2535 m in the northern Atlantic and Tropical Atlantic, in approximately one year deployments. Samplers of different thickness were used to determine the state of equilibrium POPs reached in the passive samplers. Concentrations of POPs detected in the North Atlantic near the surface (e.g. sum of 14 polychlorinated biphenyls, PCBs: 0.84 pg L^{-1}) were similar to previous measurements. At both sites, PCB concentrations showed sub-surface maxima (tropical Atlantic Ocean – 800 m, North Atlantic – 500 m). Currents seemed more important in moving POPs to deeper water masses than the biological pump. The ratio of PCB concentrations in near surface waters (excluding PCB-28) between the two sites was inversely correlated with congeners' sub-cooled liquid vapor pressure, in support of the latitudinal fractionation. The results presented here implied a significant amount of HCB is stored in the Atlantic Ocean (4.8-26 % of the global HCB environmental burdens), contrasting traditional beliefs that POPs do not reach the deep ocean.

INTRODUCTION

Open ocean seawater measurements of persistent organic pollutants (POPs) are scarce due to the difficulties associated with the sampling procedure, contamination and costs of cruises.[1] There are even less data on POPs in the deep ocean, since most of the measurements of POPs in the open ocean were limited to surface seawater. Little is known of the role played by deep ocean compartments in storing POPs from the surface.[2] Of the few previous measurements of deep oceanic POPs, two were based on active sampling, targeting polychlorinated biphenyls (PCBs) and polycyclic aromatic hydrocarbons (PAHs) in deep waters in the North Atlantic (near the South-Western edge of the Porcupine Abyssal Plain and around Iceland)[3], and PCBs in the central Arctic Basins (Nansen, Amundsen, and Makarov).[4] More recently, concentrations of PCBs, PAHs, hexachlorobenzene (HCB) and dichlorodiphenyldichloroethylene (DDE) were detected using passive sampling at 0.1-5 km depth in the Irminger Sea, the Canary Basin and the Mozambique Channel.[2] These studies reported the existence of POPs in the deeper ocean and indicated that the deep oceans could be an important compartment for storing POPs.

The study by Booij et al.[2] was the first to use passive sampling (semipermeable membrane devices, SPMDs) to study the POPs vertical distribution in the ocean. Even though active sampling has been traditionally used, it bears the disadvantage of extensive labor and extreme care of controlling blank levels.[2] Polyethylene sheets (PEs) is one common form of passive sampling devices. It has many advantages including simplicity in its chemical makeup, low cost, easy handling and a high enrichment of POPs.[5] Passive sampling was recently suggested a useful tool used monitoring POPs in open ocean.[6]

Unlike active sampling, passive samplers only take up 'truly' dissolved compounds, not those bound to colloids.

Under the circumstances that the time to reach equilibrium is not known, the sampling rate (R_s) can be used to derive the state of equilibrium upon retrieval. One way to calibrate R_s is to use performance reference compounds (PRCs). PRCs are chemicals that are artificially made which share similar properties to target compounds. However, due to the extensive long time of pre-spiking samplers with PRCs, another approach has been suggested by Bartkow et al.[7] using different thickness to confirm that equilibrium has been reached.

In this study, polyethylene passive samplers of different thickness were deployed at two deep ocean sites (eastern Fram Strait and Cape Verde Abyssal Plain) in the Atlantic Ocean to determine vertical distributions of truly dissolved concentrations of several classes of POPs, including PCBs, organochlorine pesticides (OCPs), polybrominated diphenyl ethers (PBDEs) and PAHs. The objectives of this study were to (i) measure a wide range of POPs in vertical profiles at two locations in the North Atlantic; (ii) contrast north-south and surface-to-deep gradients and (iii) improve the knowledge of fate and transport of POPs to the deep ocean.

METHODS

Sampling

PE sheet samplers preparation

PEs of three thickness were used in the study: 800, 1600 and 50μm. Polyethylene samplers preparation details are given in Supporting Information. Only 50μm PEs were pre-spiked with PRCs using the method described by Booij et al.[8]

Deep mooring sampling

Samplers were strung on stainless steel wires and attached to stainless porous cages. Cages were attached to deep mooring systems and deployed in North Atlantic (79˚ N, 4˚ E) and Tropical Atlantic (25˚ N, 38˚ W) (Figure 1). Deployment depths were 213 m, 468 m, 1173 m, 1736 m and 2535 m for the North Atlantic and 26 m, 84 m, 251 m, 800 m and 1800 m for the tropical Atlantic Ocean, respectively. Two sampling sheets were deployed at each depth. Sampling time was around one year for both deployments (North Atlantic: July 21st 2012 ~ July 8th 2013; Tropical Atlantic: Sep 14th 2012 ~ Oct 1st 2013). Current velocities were also measured at different depths by current meters during the entire mooring period. Current velocities were averaged over the deployment time for discussion in this paper. After samples were collected, they were wrapped in clean aluminum foil, shipped back to lab and stored at -4˚C until analysis.

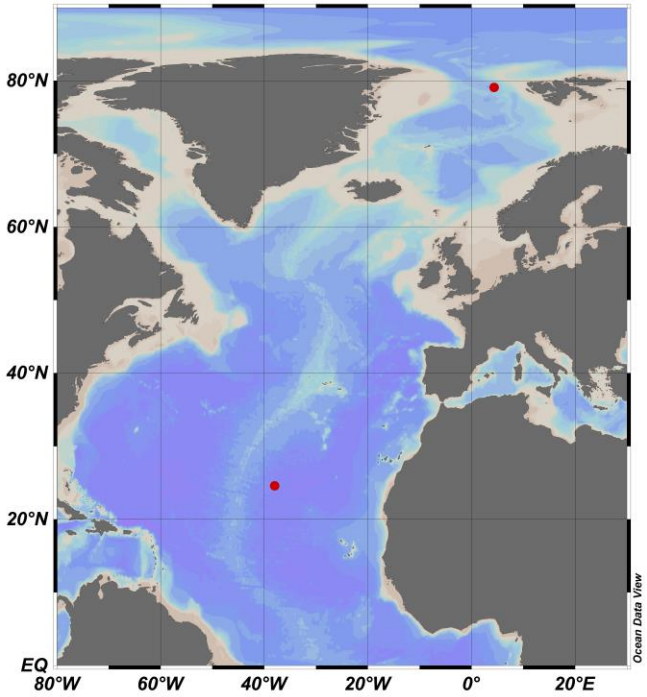

Figure 1. Sampling locations of the deep moorings in 2011-12.

Sample analysis

Sample extraction

After being wiped clean using Kimwipes, PEs were cut into pieces and extracted in hexane overnight twice with surrogate injected. Extracts were then concentrated into GC-vials and analyzed by GC-MS/ GC-MS-MS. Details on sample extraction and instrumental analysis are given in the Supporting Information.

Quality assurance/quality control

Matrix spike and lab blanks were performed for each batch of approximately 10 samples. Field blanks were taken during the North Atlantic deployment. All blanks were extracted in the same method as samples. Limits of detection (LOD) were derived from field blanks

and determined by three times the standard deviation of field blank samples. Detailed QA/QC information are in the Supporting Information (detection limits of all the compounds quantified in this study are given in Table S3; recoveries are given in Table S4).

PE concentration (C_{PE}) **conversion to environmental concentration**

Concentration of target compounds in the PEs (C_{PE}, ng g^{-1}) were converted to freely dissolved water concentrations (C_w, kg L^{-1}) by equation (1)

$$C_w = \frac{C_{PE}}{K_{PEw}} \times \frac{1}{\%\ \text{equilibrium}} \quad (1)$$

where

K_{PEw} is the compound specific partitioning coefficient between PE and water (L kg^{-1}) whose temperature correction for K_{PEw} was done using equation (2), and

%equilibrium is the percentage of equilibrium achieved by individual compound in the sampling period which is given by equation (3)

$$K_{PEw}(T) = K_{PEw}(298)\, e^{(\Delta H_{PEw}/R)\{\frac{1}{298}-\frac{1}{T}\}} \quad (2)$$

where

$K_{PEw}(T)$ and $K_{PEw}(298)$ are PEw partitioning coefficients at temperature T (K) and 298 K, respectively;

ΔH_{PEw} is the enthalpy of PEw partitioning (kJ mol^{-1});

and R is the universal gas constant (8.3143 J mol^{-1} K^{-1});

$$\%\ \text{equilibrium} = 1 - e^{(\frac{-R_s t}{K_{PEw} V_{PE}})} \quad (3)$$

where

R_s is the sampling rate (L/day) for one whole sampling sheet;

t is sampling time (days); and

V_{PE} is the volume of the PE (L).

Estimations of sampling rates

Using different thickness

Sampling rates were estimated based on the assumption that PEs deployed at the same depth/cage were exposed to the same truly dissolved concentration (C_w), and that the same sampling rate applied to all compounds. R_s pairs were assumed to be from different combinations of integers from 1~X L/day (X=100, 50, 40, 30 20, 10). For each combination, %equilibrium was calculated using equation (6) and the environmental concentration was further determined using equation (1). The aim was to find the exact pair of R_s that minimizes the total of standard deviations of all detected compounds. The total of standard deviations is defined as

$$\sum_{i=1}^{n} s_i \qquad (4)$$

where

n is the number of pairs of data, and

s is the standard deviation of the derived environmental concentration (x_j) by the two PEs in the same cage

$$s = \sqrt{\frac{1}{N-1}\sum_{j=1}^{N}(x_j - \bar{x})^2} \qquad (N=2) \qquad (5)$$

142

143 *Using PRCs*

144 Site specific sampling rates were also calculated via a nonlinear least-squares method
145 adapted from Booij and Smedes.[9] This method only applies to PEs that were pre-spiked
146 with PRCs, i.e., the 50 μm thick ones in the tropical Atlantic 84 m and 251 m deployment.

147

148 **Latitudinal Fractionation**

149 The ratio of the concentration of each individual compound near the surface layer (231
150 m) at 79˚ N divided by the surface concentration at 24˚ N (26 m) was plotted as a function
151 of their subcooled liquid vapor pressure (P_L).

152

153 **Estimation of water age using chlorofluorocarbons, CFCs**

154 Transient tracers, including CFCs, are useful as a water mass tracer because their
155 atmospheric concentration can be uniquely related to a calendar year. In turn, water at the
156 ocean surface records this unique concentration based upon air-water gas partitioning. The
157 equilibrium partitioning between CFC concentration in the air and water is described by
158 Henry's Law. Dissolved CFCs concentration C_w (mol kg^{-1}) at the locations of interest were
159 obtained from Carbon Hydrographic Data Office (CCHDO). Temperature and salinity data
160 were obtained from the same origin and were used for deriving the Henry's Law Constant
161 H (mol kg^{-1}). The molar ratio of CFCs in the atmosphere χ (mol CFC mol^{-1} air) were then
162 calculated using

163 $$\chi = \frac{C_w}{H} \qquad (6)$$

164 The results represented the molar ratio of CFCs in the atmosphere when the water were
165 at the surface. They were compared to recorded atmospheric CFCs concentrations from
166 Carbon Dioxide Information Analysis Center (CDIAC) to determine the calendar year
167 when the water was last contact with the air.[10] SF_6 data were of the highest priority if
168 available; if not, CFC-12 data were used instead.
169

170 **RESULTS AND DISCUSSION**

171 **Truly dissolved surface concentrations of POPs**

172 *Tropical Atlantic*

173 $\sum_{14}$PCBs concentrations near the surface of the tropical Atlantic (Cape Verde Abyssal
174 Plain) were 8.5 pg L^{-1} (Table S12), with $\sum_{ICES}$PCBs (PCB-28, 52, 90/101, 118, 138,153
175 and 180) of 6.2 pg L^{-1}; they constituted ~73% of all the $\sum_{14}$PCBs detected. $\sum_{14}$PCBs was
176 close to the high end of reported value of ($\sum_{27}$PCBs , 0.24-5.7 pg L^{-1}) by Gioia et al.[11] but
177 lower than the measurement ($\sum_{36}$PCBs North Atlantic, 26 pg L^{-1}) by Iwata et al.[12]
178 $\sum_{ICES}$PCBs was larger than (mean 2.5 pg L^{-1}) by Lohmann et al.[13] and (0.071-1.7 pg L^{-1})
179 by Gioia et al.[11]

180 HCB concentration was found at 6.0 pg L^{-1} near surface, higher than what was found in
181 the North Atlantic (0.1-3 pg L^{-1}) by Lohmann et al.[13] but within the range of Northern
182 Hemisphere average (2-9 pg L^{-1}) by Booij et al.[14] *p,p′*-DDT, *o,p′*-DDT and *p,p′*-DDE were
183 all within the range of 0.2-0.5 pg L^{-1}, which was in agreement with North Atlantic (0.1-3
184 pg L^{-1}) by Lohmann et al.[13] and close to the lower end of Northern Hemisphere average
185 (0.3-1.4 pg L^{-1}) by Booij et al.[14] and detected near 30˚N Atlantic (0.5 pg L^{-1}) by Iwata et
186 al.[12]

187 The only detectable PBDEs were 47, 100 and 99. Concentrations were 1.4, 0.3 and 1.6
188 pg L^{-1}, slightly higher than (~ 0.5 pg L^{-1} for 47 and around 0.1 pg L^{-1} for 99 and 100) by
189 Lohmann et al.[15] and (0.02-1.05, nd-0.11 and 0.01-0.53 pg L^{-1} respectively) by Xie et al.[16]
190 Detected $\sum_7$PAHs was 83 pg L^{-1} near surface at the tropical Atlantic. This is within the
191 range ($\sum_{10}$PAHs, 58-1070 pg L^{-1}) reported by Nizzetto et al.[17] near the northwest coast of
192 Africa, which was potentially influenced by emerging oil industry, biomass burning and
193 natural source of PAHs in Africa. PAH concentrations measured here were lower than
194 ($\sum_3$PAHs , average of 270 pg L^{-1}) by Lohmann et al.[18] near the coast of North America. As
195 to individual PAHs, phenanthrene, fluoranthene and pyrene were dominant, which is in
196 agreement with other studies.[17,18]
197
198 *North Atlantic*
199 In the North Atlantic (Fram Strait), surface ∑PCBs concentration of the dissolved phase
200 was 0.8 pg L^{-1} in this study (Figure 3 & Table S12), which was comparable to what was
201 observed for $\sum_7$PCBs (0.7 pg L^{-1})[4] and $\sum_6$PCBs (< 1 pg L^{-1})[19]. As for individual congeners,
202 the highest concentration was determined by PCB-28, followed by 18, 44, 52 and then 101,
203 138, 153. This result is in agreement with result from Gioia et al.[19] PCB-18, 28, 52, 101,
204 118, 138, 153 were the most detected congeners in previous studies; they were also the
205 dominant PCBs in this study.
206 HCB was the OCP detected at the highest concentration. The near surface concentration
207 was 10 pg L^{-1}, higher than those reported from the North Atlantic Bloom Experiment
208 (NABE)[20] but close to results from the RV Polarstern cruise ARK-XX (high Arctic , 4-10
209 pg L^{-1}),[21] results for the East Atlantic Ocean (2-9 pg L^{-1})[14] and for the Arctic Ocean (7 pg

210 L^{-1}).[22] It was mentioned by Lohmann et al.[21] that $[HCB]_{diss}$ was negatively correlated with
211 water temperature (T_w): $[HCB]_{diss} = 6.4\text{-}0.57\times T_w$. Considering the higher averaged
212 temperature from the NABE study (10 °C), $[HCB]_{diss}$ was close to the other reported values
213 after temperature corrections.

214 There were no HCHs detected, possibly due to the less hydrophobic nature of HCHs
215 which reduced their uptake by PEs. *p,p′*-DDE and *p,p′*-DDD are two breakdown products
216 of *p,p′*-DDT. Their concentrations were around 0.1-0.4 pg L^{-1}, which were also close to
217 previous studies.[20,21] *p,p′*-DDT concentration was lower than *p,p′*-DDE and *p,p′*-DDD,
218 indicating that there is no new source of *p,p′*-DDT to the central Arctic Basin.

219 The only PBDEs detected were BDE-99 and BDE-100. Surface seawater concentrations
220 in the dissolved phase were 0.4 pg L^{-1} and 0.025 pg L^{-1}, respectively. Concentrations were
221 similar to those observed in the Asian Arctic by Möller et al.[23] While BDE-47 was one of
222 the dominant PBDEs in the other studies, it was not detected in Fram Strait (this study).

223 ∑PAHs was 148 pg L^{-1}, higher than (16-65 pg L^{-1}) by Schulz-Bull et al.[24] PAH
224 compounds detected tend to vary among studies conducted at different regions. Among all
225 the PAHs, fluoranthene was the one more consistently detected. Concentration of
226 fluoranthene at 213 m (94 pg L^{-1}) in this study fell in the range of other studies [2,21] in the
227 same region.

228 In summary, the concentrations of various POPs near the surface of the tropical and
229 northern Atlantic were in agreement with previous measurements reported for the remote
230 Atlantic. Comparisons (sampling year, sampling location, etc) are summarized in Table
231 S13. Overall, the comparison validates the use of PE samplers and the derived
232 concentrations.

A detailed discussion on the certainty of estimated concentrations can be found in the Supporting Information.

Latitudinal fractionation

Next, we investigated whether there are large scale trends in PCB profiles reflecting global processes. As our sampling sites are not directly linked by one major current, any differences in PCB profiles should mainly stem from atmospheric deposition to the surface ocean. As discussed in the methods, linear regression was used to investigate whether there was a trend of the ratio of the compounds detected at the two sites and their physico-chemical properties. Results are given in Figure 2. The overall correlation was not strong ($R^2 = 0.25$, p-value = 0.25), due to an outlier (PCB-28). An outlier was defined as a value outside of 1.5 times of interquartile distance (IQD = Q3-Q1) subtracted from or added to the first quartile (Q1) and the third quartile (Q3).[25] A significant higher concentration of PCB-28 in the north could be resulted from an unknown emission source near the sampling area. After removing PCB-28, the correlation between north-south ratio of POP concentrations and log P_L was much improved ($R^2 = 0.95$) and became significant (p-value = 0.001). The results imply that higher mobility compounds (higher log P_L) display a relatively greater abundance up north than compounds with lower mobility. This supports the ideas formulated in the cold condensation theory, driven by large-scale atmospheric transport.[26] Our results agreed with an increasing trend of concentration ratios of PCBs (88˚ N : 62˚ N) along with log vapor pressure observed by Sobek and Gustafsson.[27] We note, however, that the two samples we used for the comparison were not real surface samples, especially for North Atlantic site.

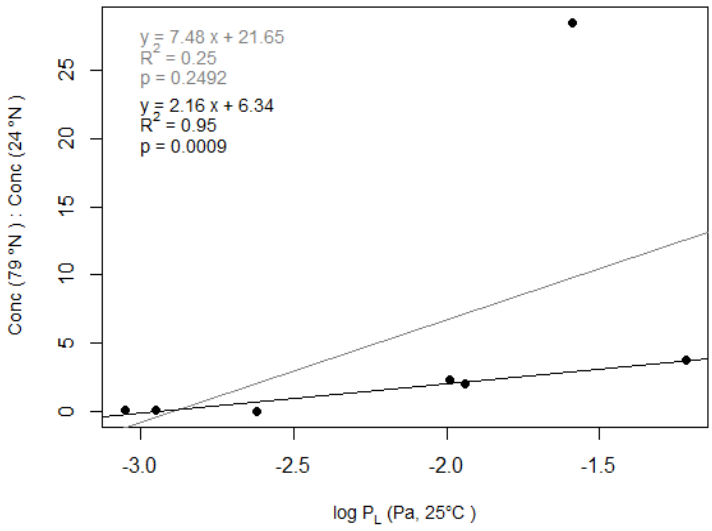

Figure 2. Ratio of the concentration at 79˚ N and 24˚ N for PCBs detected at the depth nearest to the surface at both sites, as a function of log sub-cooled liquid vapor pressure (Pa) at 25˚C (Table S2). (Grey: all detected PCBs; Black: PCB-28 removed)

Depth profile - comparison with the other deep ocean POP measurements

Depth profiles were plotted as in Figure 3 (values are given in Table S12). Comparisons were made with the other two studies: Booij et al.[2] and Schulz-Bull et al[24]. Good agreement was achieved between the three studies. In the tropical Atlantic Ocean, most dissolved PCBs were detected at ~100 fg/L level with a few major PCBs (e.g. PCB-101,118, 153,138) detected at concentrations larger than 1,000 fg/L, HCB at around 6,000 fg/L and PAHs within 1-200 fg/L . In the North Atlantic Ocean, PCBs were at ~100 fg/L, HCB at ~10,000 fg/L in the upper water column and PAHs within 1-100 pg/L (North Atlantic). Details are given in Table S14.

Depth profile - Tropical Atlantic site

Depth profile shapes

PCBs, OCPs and PAHs congeners displayed similar depth profiles; mostly with a maximum at 800 m. Vertical profiles for PBDE are significantly different from the other compounds. All BDEs congeners exhibited a drastic decline in truly dissolved concentrations below ~250 m. Little BDEs were detected at depth, possibly linked to the fact that production of BDEs peaked 20~30 years later than those for PCBs and OCPs. Thus, PCBs and OCPs had more time to penetrate the deeper layers of the oceans, while PBDEs have only touched the surface ocean.

Explanations for depth profile

No measurements were done above 1400 m at the Canary Basin site of Booij et al.[2] and due to the similar concentrations found near the surface at other locations in the Atlantic, the authors concluded that no large concentration gradients existed in the upper 1400 m at Canary Basin. However, in the present study, a concentration maximum existed at 800 m which was significantly different from the other depths. We note that neither study was able to fully resolve depth profiles satisfactorily as only a few samplers were deployed, potentially missing important vertical features in POPs concentration. In the present study, sampling depths were restricted to specific coupling points in the mooring line, thus we were not able to add more in addition to the present stations.

Two reasons were investigated to explain the shapes of the PCBs, OCPs and PAHs depth profiles: i) Particle binding/sinking; and ii) Water current transport. Chemicals with higher K_{ow} (partitioning coefficient between octanol and water) tend to bind to particles more strongly. With particles sinking and getting remineralized in the deep ocean, POPs are

295 released back into the water. PCBs, for instances, have different levels of chlorination and
296 those with high chlorination degrees have higher tendency to bind to particles. The
297 composition from different PCBs chlorination groups were plotted in Figure S3. There is
298 an increase of di- and tri-PCBs with depth, particularly at 800 m and below. No trend of
299 increasing contribution from higher chlorinated-PCBs can be seen, suggesting that particle
300 binding/sinking processes did not dominate the 800 m maximum in PCB concentrations.
301 We note that greatest concentrations of hexa- and hepta-chlorinated congeners were found
302 in the surface samples of the tropical Atlantic, not at depth. Once exported from the surface
303 Ocean, photodegration will not affect PCBs any longer. There is little evidence that
304 biodegradation has affected PCBs, in light of concentrations profiles with depth that are
305 not decreasing. Booij et al.[2] also pointed out that particle-associated transport is
306 insignificant in transferring contaminants to the deep ocean.

307 The existence of Mediterranean water has been observed in East Atlantic.[28]
308 Mediterranean water sinks and mixes with Eastern Atlantic water after it flows out of the
309 Strait of Gibraltar, reaches equilibrium around 1000 m in depth and spreads across the
310 North Atlantic. So-called 'Meddies' are anticyclonic rings that were formed after
311 Mediterranean water flows out of the Strait of Gibraltar. They are 100 km in diameter and
312 800 m in thickness and could last as long as two or more years. It was estimated that some
313 25% of the Mediterranean outflow originates in Meddies and this makes Meddies one tool
314 to trace Mediterranean water.[29] Meddies are normally associated with temperature and
315 salinity anomalies, resulting from the warmer, saltier and younger feature of Mediterranean
316 water. Figure S5 is the vertical section along East Atlantic. There is anomaly at 24.58˚N,
317 800 m in depth in all vertical profiles in Figure S5. Temperature, salinity and CFC-11 data

indicated a ring of warmer, saltier and younger water mass than surroundings. Although our sampling location was not exactly the same as where the anomaly occurred, considering the size of Meddies and the close proximity of these two locations, intruding from Mediterranean water cannot be ruled out.

Another evidence towards the influence of Mediterranean water on the sampler at 800 m in depth is the comparison to reported POPs in the Mediterranean water. From the study conducted in 2006-2007, concentrations in seawater were reported as $\sum_{41}$PCBs 2-84 pg L^{-1} and HCB up to 1.7 pg L^{-1} in the Mediterranean Sea and Black Sea.[30] The importance of penta- and hexa-chlorinated biphenyls were in agreement with tropical Atlantic samples reported here. Reported concentration of HCB in coastal water of Alexandria, Egypt were much higher (surface water: 27 pg L^{-1}).[31]

The implication from our results is that the upper 1800 m of the water column was not well mixed with respect to POPs concentrations, and there were multiple water layers which potentially had different water mass origins, possibly affecting POPs concentrations and profiles.

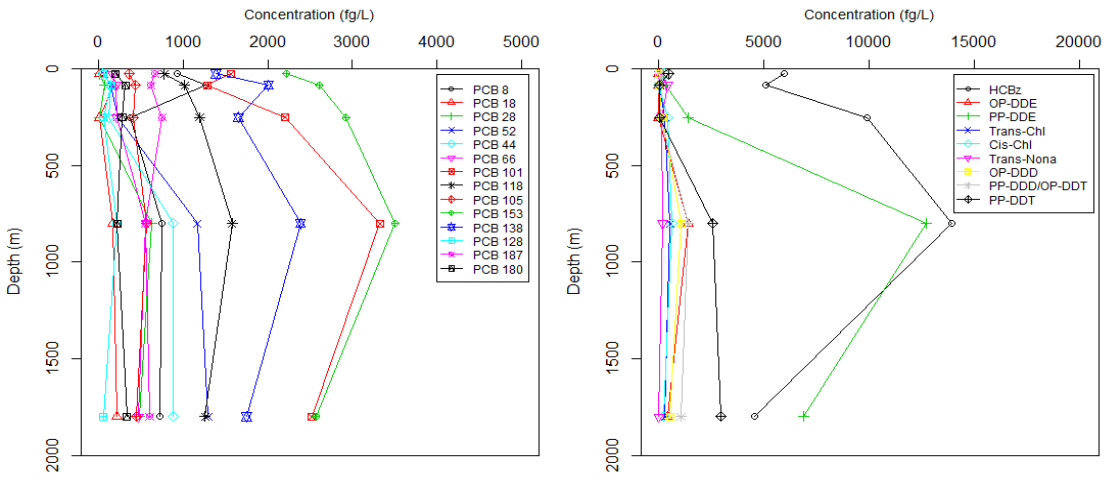

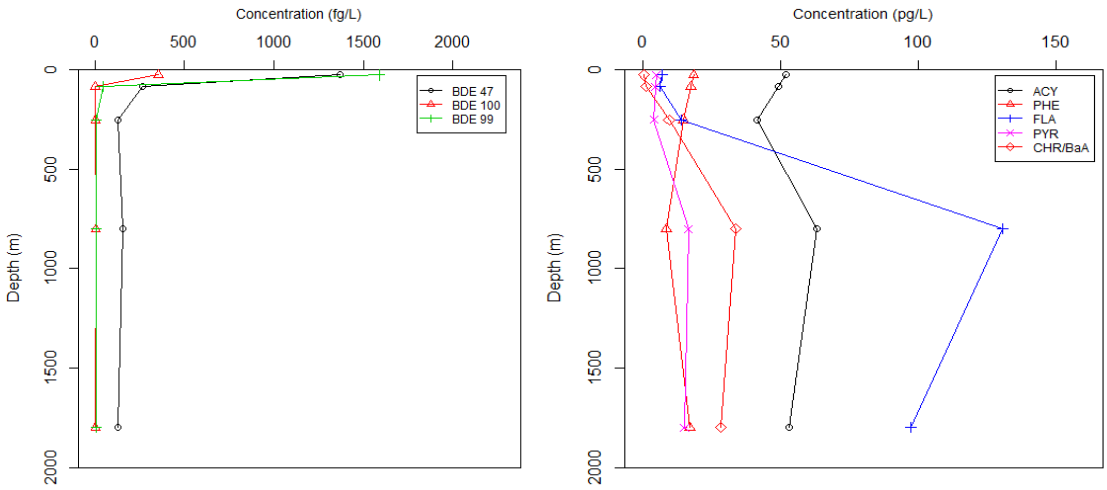

Figure 3. Depth profiles of POPs (PCBs, OCPs, PBDEs and PAHs) in the tropical Atlantic. Lines are for connecting points only and do not represent any measurements.

Depth profile - North Atlantic site

Depth Profile Shapes

Depth profiles were plotted as in Figure 4 (values are given in Table S12). Most compounds showed similar depth profiles, such as PCBs, HCB and BDE 99. They exhibited a general decrease trend towards the deep and some maximum concentration appearing at 500 m in depth. Decreasing profiles of PCBs[3,24] and PAHs[24] were observed in the 1990s in North Atlantic, while a nutrient-like profile was shown recently addressing the importance of advective flow-off from the continental shelf.[4] The distribution pattern observed in this study neither follows a decreasing nor an increasing trend. Different distribution patterns observed for the other compounds can be partly explained by their separate degradation processes and emission pathways.

Explanations for depth profile

Similar to the discussion above, particle binding and sinking origination was tested by PCBs chlorination composition plotted in Figure S3. Compared to the results from the tropical Atlantic site, smaller degrees of chlorination tend to yield larger contribution of the ∑PCBs in the North Atlantic, which means the contribution from each group has the order of tri- > tetra- > penta- > hexa- . This composition pattern of chlorinated groups are in line with other studies.[4,19] No significant fraction of higher chlorinated PCBs was observed along depth, indicating that particle sinking was not a major contributor to the PCBs in depth in North Atlantic either.

The Fram Strait is the pathway for water exchange between the North Atlantic and the Arctic Basin. Warm and saline Atlantic water flows into the Arctic Ocean at the eastern side of Fram Strait; cold Arctic water flows out of the Arctic Mediterranean in the western Fram Strait. Different branches of the Norwegian Atlantic Current (NwAC) converge and form the West Spitsbergen Current (WSC). A significant part does not enter the Arctic Ocean, mixes with the outflowing Arctic water and recirculates into the Nordic Seas.[32] The deep mooring site in this study was influenced by these recirculation water masses. From 1997 onwards, a deep oceanographic mooring array at 78˚50'N[33] as well as three individual moorings at the LTER (Long-Term Ecological Research) observatory HAUSGARTEN[34] were maintained in the Fram Strait. From the mooring data, it was noticed that deep water (~ 2500 m deep) in the plateau area near the Fram Strait Sill (~ 0˚ E) reflects mixing properties from two end members: the Greenland Sea Deep Water (GSDW) and the Eurasian Basin Deep Water (EBDW); at mooring site HG-IV (central HAUSGARTEN site), the water near bottom is almost purely EBDW. The mean flow at HG-IV is locally topographically steered but does not achieve the cross sill advection.[35] Unlike the Tropical

374 Atlantic sampling site, it is hard to derive the water mass origins for certain depths at the
375 North Atlantic sampling site due to the complexity and vigorousness in the water mixing
376 processes.

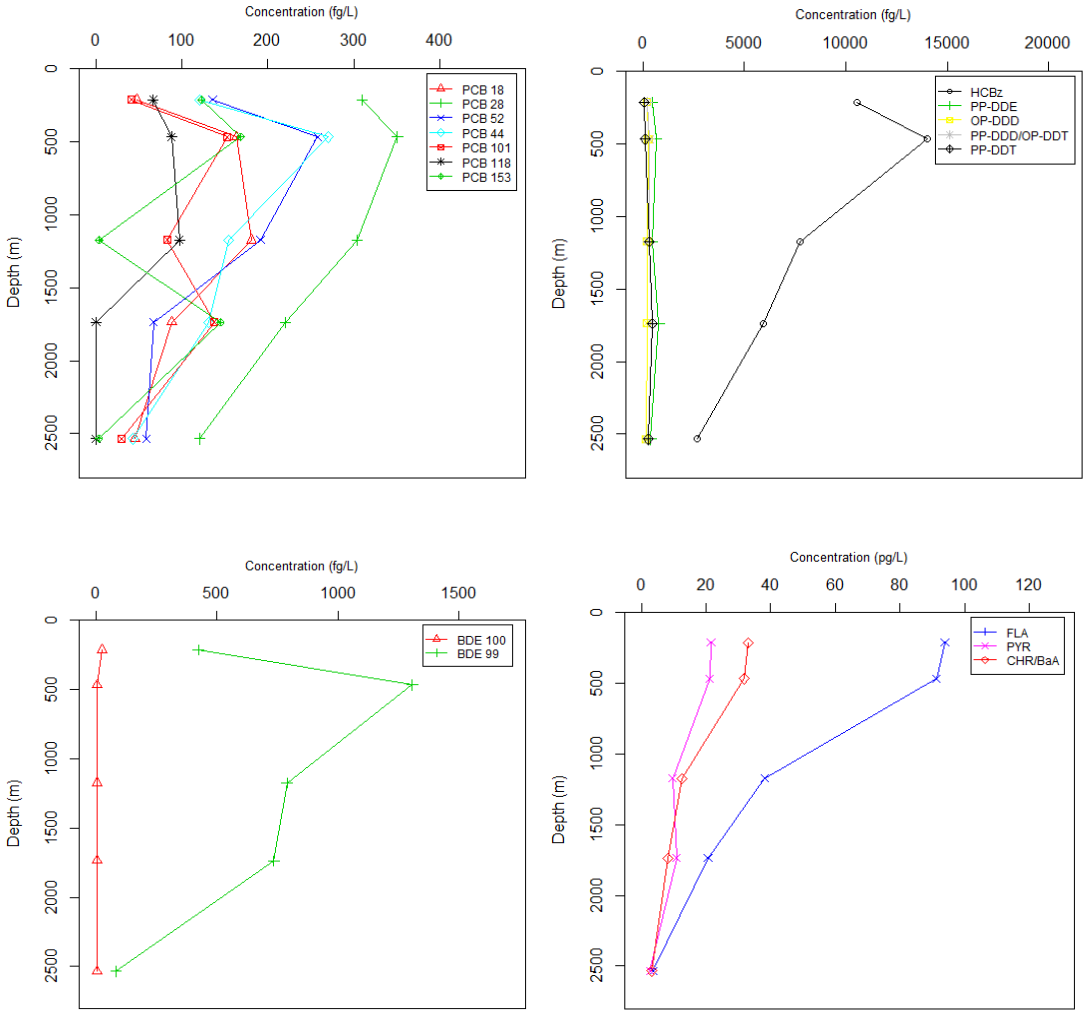

377

378

379 **Figure 4.** Depth profiles of POPs (PCBs, OCPs, PBDEs and PAHs) in the North Atlantic.
380 Lines are for connecting points only and do not represent any measurements.

381

382 **CFCs ventilation ages and plots against PCBs profiles**

383 *Tropical Atlantic*

There was no available SF_6 data for tropical Atlantic close to our deployment period; CFC-12 data were used instead to assess water mass origin and age. CFC-12 derived ventilation age was plotted against the ∑PCBs in Figure S4. Detailed information for ventilation age calculation was given in Table S15. The three sites chosen from CCHDO for the tropical Atlantic gave close CFC-12 data throughout the water column, indicating little variance of water composition around (24˚ N, 38˚ E). Ventilation age was then derived by averaging out the available ventilation age from SITE1 to SITE 3 (Table S15).

The concentration maximum of ∑PCBs had a ventilation age of around 40 years, coinciding with the peak in PCBs emission in the 1970s.[36] However, some other depths that were not sampled may exhibit larger ∑PCBs than 800 m. It is also unknown whether there is a lag in the response time of oceanic POPs to global emission, and how long it might be. As discussed previously, the peak in PCB concentrations at 800 m could also be due to Mediterranean water masses. Therefore, we conclude here that ∑PCBs detected at the tropical Atlantic site generally followed the emission history of PCBs; yet it is unclear whether the 800 m maximum reflected the 1970s PCBs emission peak.

North Atlantic

SF_6 data was used for deriving the ventilation age of water masses in the North Atlantic. Large variations occurred between different sites chosen for the SF_6 data, most probably resulting from the complexity in bathymetric and water current conditions in this area. The closest sampling SF_6 location to our PE sampling site which also covers the whole PE sampling depths was included in Table S15. Figure S4 indicated a maximum in ∑PCBs at a ventilation age of ~10-20 years, younger than the maximum at tropical Atlantic site.

Again, due to the limited data points, it is hard to accurately determine where the ∑PCBs maximum would occur. The overall distribution pattern of ∑PCBs with ventilation age still followed the global emission pattern, with one peak in the middle and decrease on both sides. The shift in the concentration peak of ~20 years could be an oceanic POPs response time lag not captured by the tropical Atlantic site measurement.

Mass balance implications for POPs in the Ocean

We selected HCB for calculating mass balance in the Atlantic Ocean because the vertical profiles reported here show no significant difference in absolute concentrations across the Atlantic Ocean and the trend is similar. However, for PCBs, OCPs (other than HCB), PBDEs and PAHs either the concentration or the trend lacks consistency between the two sampling sites.

For HCBs, we assumed a uniform spatial distribution across the Atlantic Ocean. Pilson[37] estimated the whole surface area of Atlantic as 8.65×10^7 km^2 with average depth of 3,700 m. The upper ocean (0-1,200 m) is loaded with HCB at a concentration of 9.6 ± 3.5 pg L^{-1} (mean ± standard deviation), while the deep ocean (1,200-3,700 m) has a concentration of 4.4 ± 1.6 pg L^{-1}, based on the results of this work. The total amount of HCB residing in the Atlantic Ocean is 1,947 ± 709 t; it accounted for 45 ± 16% of the total HCB stored in the ocean if using the estimation from Barber et al (4,300 t).[38] The total global production of HCB was estimated as >100,000 t.[39] The contemporary environmental burden of HCB was calculated as 10,000-26,000 t.[38] Hence, the Atlantic Ocean stores less than 2.6 % of HCB ever produced, but contains 4.8-26 % of the global HCB environmental burdens.

IMPLICATION

The current study confirmed that it is possible to deploy passive samplers to determine vertical POPs gradients in the Oceans. Yet deployment times of around 1 year were insufficient for most POPs to reach equilibrium in 800 and 1,600 um thick sheets. The slow equilibration was in part due to the need to use deployment cages to guarantee safe deployment and retrieval of passive samplers. We were able to constrain sampling rates by combining results from different thicknesses, PRC-laden sheets and modeling. Future deployments would benefit from more PRC-impregnated samplers to derive in situ sampling rates.

Results from this study supported previous work in highlighting the important role of deep ocean as a compartment storing POPs. The presence of numerous POPs in deeper water suggests that the deep ocean carries a significant mass already, particularly of the legacy POPs. An intriguing observation from the two sites considered here is that lateral water mass transport might be more important than vertical POP transport on settling particles. As an example, PBDEs had penetrated the deep water masses of the Atlantic Ocean to a much smaller degree than the legacy PCBs and OCPs. Clearly, additional work, ideally both at numerous sites and with greater vertical resolution could help constrain the importance of water mass versus particle-bound transport of POPs to depth.

ASSOCIATED CONTENT

Supporting Information

Additional details related to the physicochemical constants, sampling setup, instrumental analysis, quality control and CFC information are available. This material is available free of charge via the Internet at http://pubs.acs.org.

AUTHOR INFORMATION

Corresponding Author

*E-mail: lohmann@gso.uri.edu; Tel 401-874-6612; fax 401-874-6811

Author Contributions

The manuscript was written through contributions of all authors. All authors have given approval to the final version of the manuscript.

Notes

The authors declare no competing financial interest.

ACKNOWLEDGMENTS

We acknowledge funding from the National Science Foundation (ARC 1203486) to study the transport of POPs into the Arctic Ocean. We thank J. Thomas Farrar (WHOI) for sampler deployment and current data at the tropical Atlantic site, Brice Loose (URI) for assistance with CFC data, and the ship's crew and of Normen Lochthofen for the deployment and recovery of the mooring in Fram Strait during R/V Polarstern cruise ARK-XXVII/2. This is publication e39092 of the Alfred-Wegener-Institut Helmholtz-Zentrum für Polar- und Meeresforschung, Germany.

REFERENCES

(1) Gioia, R.; Dachs, J.; Nizzetto, L.; Lohmann, R.; Jones, K. C. Atmospheric Transport , Cycling and Dynamics of Polychlorinated Biphenyls (PCBs) from Source Regions to Remote Oceanic Areas. In *Occurrence, Fate and Impact of Atmospheric Poluutants on Environmental and Human Health, ACS Symposium Series*; L. McConnell, J. Dachs, C. J. H., Ed.; 2013; Vol. 1149 (**ISBN13:** 9780841228900, **eISBN:** 9780841228917), pp 3–18.

(2) Booij, K.; Bommel, R. Van; Aken, H. M. Van; Haren, H. Van; Brummer, G. A.; Ridderinkhof, H. Passive sampling of nonpolar contaminants at three deep-ocean sites. *Environ. Pollut.* **2014**, *195*, 101–108.

(3) Schulz, D. E.; Petrick, G.; Duinker, J. C. Chlorinated biphenyls in North Atlantic surface and deep water. *Mar. Pollut. Bull.* **1988**, *19* (10), 526–531.

(4) Sobek, A.; Gustafsson, Ö. Deep water masses and sediments are main compartments for polychlorinated biphenyls in the Arctic Ocean. *Environ. Sci. Technol.* **2014**, *48* (12), 6719–6725.

(5) Lohmann, R. A critical review of low-density polyethylene's partitioning and diffusion coefficients for trace organic contaminants and implications for its use as a passive sampler. *Environ. Sci. Technol.* **2012**, *46*, 606–618.

(6) Lohmann, R.; Muir, D. Global aquatic passive sampling (AQUA-GAPS): Using passive samplers to monitor POPs in the waters of the world. *Environ. Sci. Technol.* **2010**, *44* (3), 860–864.

(7) Bartkow, M. E.; Hawker, D. W.; Kennedy, K. E.; Müller, J. F. Characterizing Uptake Kinetics of PAHs from the Air Using Polyethylene-Based Passive Air Samplers of Multiple Surface Area-to-Volume Ratios. *Environ. Sci. Technol.* **2004**, *38* (9), 2701–2706.

(8) Booij, K.; Smedes, F.; Van Weerlee, E. M. Spiking of performance reference compounds in low density polyethylene and silicone passive water samplers. *Chemosphere* **2002**, *46*, 1157–1161.

(9) Booij, K.; Smedes, F. An improved method for estimating in situ sampling rates of nonpolar passive samplers. *Environ. Sci. Technol.* **2010**, *44* (17), 6789–6794.

(10) Bullister, J. Atmospheric CFC-11, CFC-12, CFC-113, CCl4 and SF_6 Histories (1910-2014) http://cdiac.ornl.gov/oceans/new_atmCFC.html (accessed Jun 10, 2015).

(11) Gioia, R.; Nizzetto, L.; Lohmann, R.; Dachs, J.; Temme, C.; Jones, K. C. Polychlorinated Biphenyls (PCBs) in Air and Seawater of the Atlantic Ocean: Sources, Trends and Processes. *Environ. Sci. Technol.* **2008**, *42* (5), 1416–1422.

(12) Iwata, H.; Tanabe, S.; Sakai, N.; Tatsukawa, R. Distribution of Persistent Organochlorines in the Oceanic Air and Surface Seawater and the Role of Ocean on Their Global Transport and Fate. *Environ. Sci. Technol.* **1993**, *27* (6), 1080–1098.

(13) Lohmann, R.; Klanova, J.; Kukucka, P.; Yonis, S.; Bollinger, K. PCBs and OCPs on a east-to-west transect: The importance of major currents and net volatilization for PCBs in the atlantic ocean. *Environ. Sci. Technol.* **2012**, *46*, 10471–10479.

(14) Booij, K., van Bommel, R., Jones, K.C., Barber, J. L. Air-water distribution of hexachlorobenzene and 4,40-DDE along a North-South Atlantic transect. *Mar. Pollut. Bull.* **2007**, *54* (6), 814–819.

(15) Lohmann, R.; Klanova, J.; Kukucka, P.; Yonis, S.; Bollinger, K. Concentrations, fluxes, and residence time of PBDEs across the tropical Atlantic Ocean. *Environ. Sci. Technol.* **2013**, *47*, 13967–13975.

(16) Xie, Z.; Möller, A.; Ahrens, L.; Sturm, R.; Ebinghaus, R. Brominated flame retardants in seawater and atmosphere of the Atlantic and the southern ocean. *Environ. Sci. Technol.* **2011**, *45* (5), 1820–1826.

(17) Nizzetto, L.; Lohmann, R.; Gioia, R.; Jahnke, A.; Temme, C.; Dachs, J.; Herckes, P.; Guardo, A. Di; Jones, K. C. PAHs in Air and Seawater along a North–South Atlantic Transect: Trends, Processes and Possible Sources. *Environ. Sci. Technol.* **2008**, *42* (5), 1580–1585.

(18) Lohmann, R.; Klanova, J.; Pribylova, P.; Liskova, H.; Yonis, S.; Bollinger, K. PAHs on a west-to-east transect across the tropical Atlantic Ocean. *Environ. Sci. Technol.* **2013**, *47* (6), 2570–2578.

(19) Gioia, R.; Lohmann, R.; Dachs, J.; Temme, C.; Lakaschus, S.; Schulz-Bull, D.; Hand, I.; Jones, K. C. Polychlorinated biphenyls in air and water of the North Atlantic and Arctic Ocean. *J. Geophys. Res.* **2008**, *113* (D19), D19302.

(20) Zhang, L.; Bidleman, T.; Perry, M. J.; Lohmann, R. Fate of chiral and achiral organochlorine pesticides in the north Atlantic bloom experiment. *Environ. Sci. Technol.* **2012**, *46*, 8106–8114.

(21) Lohmann, R.; Gioia, R.; Jones, K. C.; Nizzetto, L.; Temme, C.; Xie, Z.; Schulz-Bull, D.; Hand, I.; Morgan, E.; Jantunen, L. Organochlorine pesticides and PAHs

in the surface water and atmosphere of the North Atlantic and Arctic Ocean. *Environ. Sci. Technol.* **2009**, *43* (15), 5633–5639.

(22) Strachan WMJ, Fisk A, Teixeira CF, Burnsiton DA, N. R. PCBs and organochlorine pesticide concentrations in the waters of the Canadian Archipelago and other Arctic regions (Abstract 13). In *Proceedings of the Workshop on persistent organic pollutants (POPs) in the Arctic: Human health and environmental concerns.*; AMAP report: Arctic Monitoring and Assessment Program: Rovaniemi Finland, 2000.

(23) Möller, A.; Xie, Z.; Cai, M.; Zhong, G.; Huang, P.; Cai, M.; Sturm, R.; He, J.; Ebinghaus, R. Polybrominated diphenyl ethers vs alternate brominated flame retardants and dechloranes from East Asia to the arctic. *Environ. Sci. Technol.* **2011**, *45* (16), 6793–6799.

(24) Schulz-Bull, D. E.; Petrick, G.; Bruhn, R.; Duinker, J. C. Chlorobiphenyls (PCB) and PAHs in water masses of the northern North Atlantic. *Mar. Chem.* **1998**, *61* (1-2), 101–114.

(25) Tukey, J. W. *Exploratory data analysis.*; Addison-Wesley, 1977.

(26) Wania, F.; Mackay, D. Peer reviewed: tracking the distribution of persistent organic pollutants. *Environ. Sci. Technol.* **1996**, *30*, 390A – 6A.

(27) Sobek, A.; Gustafsson, O. Latitudinal fractionation of polychlorinated biphenyls in surface seawater along a 62 degrees N-89 degrees N transect from the southern Norwegian Sea to the North Pole area. *Environ. Sci. Technol.* **2004**, *38* (10), 2746–2751.

(28) Martí, S.; Bayona, J. M.; Albaigés, J. A Potential Source of Organic Pollutants into the Northeastern Atlantic: The Outflow of the Mediterranean Deep-Lying Waters through the Gibraltar Strait. *Environ. Sci. Technol.* **2001**, *35* (13), 2682–2689.

(29) Knauss, J. A. *Introduction to physical oceanography*, 2nd ed.; Waveland Press, Inc., 2005.

(30) Berrojalbiz, N.; Dachs, J.; Del Vento, S.; Ojeda, M. J.; Valle, M. C.; Castro-Jiménez, J.; Mariani, G.; Wollgast, J.; Hanke, G. Persistent organic pollutants in mediterranean seawater and processes affecting their accumulation in plankton. *Environ. Sci. Technol.* **2011**, *45* (10), 4315–4322.

(31) Abd-Allah, A. M. A. Organochlorine contaminants in microlayer and subsurface water of Alexandria Coast, Egypt. *J AOAC Int* **1999**, *82*, 391–398.

(32) Schauer, U.; Fahrbach, E.; Osterhus, S.; Rohardt, G. Arctic warming through the Fram Strait: Oceanic heat transport from 3 years of measurements. *J. Geophys. Res.* **2004**, *109* (6), 1–14.

(33) A. Beszczynska-Möller, E. Fahrbach, U. Schauer, E. H. Variability in Atlantic water temperature and transport at the entrance to the Arctic Ocean 1997–2010. *ICES J. Mar. Sci.* **2012**, *69*, 852–863.

(34) Soltwedel, T.; Bauerfeind, E.; Bergmann, M.; Bracher, A.; Budaeva, N.; Busch, K.; Cherkasheva, A.; Fahl, K.; Grzelak, K.; Hasemann, C.; et al. Natural variability or anthropogenically-induced variation? Insights from 15 years of multidisciplinary observations at the Arctic open-ocean LTER site HAUSGARTEN. *Ecol. Indic.* **2016**, *65*, 89-102.

(35) Appen, W.-J. Von; Schauer, U.; Cabrillo, R. S.; Bauerfeind, E.; Beszczynska-Möller, A. Exchange of warming deep waters across Fram Strait. *Deep Sea Res. Part I* **2015**, *103*, 86–100.

(36) Jones, K. C.; Barber, J. L.; Booij, K.; Jaward, F. M. Evidence for dynamic air-water coupling of persistent organic pollutants over the open Atlantic Ocean. *Environ. Sci. Technol.* **2004**, *38*, 2617–2625.

(37) E.Q.Pilson, M. *An introduction to the chemistry of the sea*, 2nd ed.; Cambridge University Press, 2013.

(38) Barber, J. L.; Sweetman, A. J.; Van Wijk, D.; Jones, K. C. Hexachlorobenzene in the global environment: Emissions, levels, distribution, trends and processes. *Sci. Total Environ.* **2005**, *349* (1-3), 1–44.

(39) ATSDR. Toxicological profile for HCB. US Department of Health and Human Services, Public Health Service, Agency for Toxic Substances and Disease Registry (ATSDR); Atlanta, GA, 1997.

TOC Art

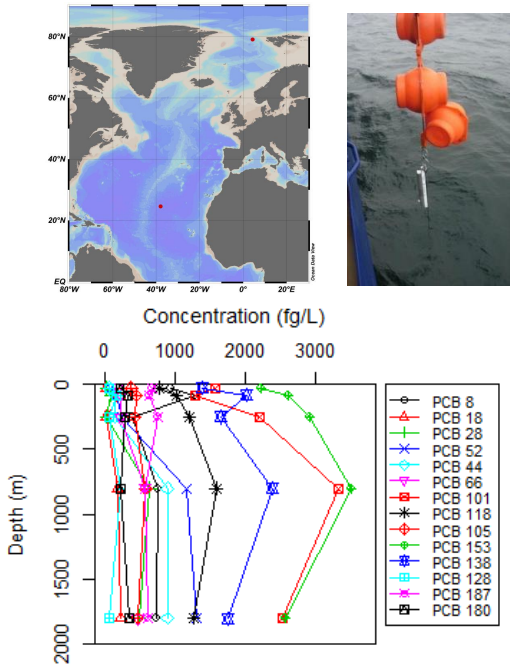
80°N
60°N
40°N
20°N
EQ
80°W
60°W
40°W
20°W
0°
20°E
Concentration (fg/L)
0
1000
2000
3000
Depth (m)
0
500
1000
1500
2000
PCB 8
PCB 18
PCB 28
PCB 52
PCB 44
PCB 66
PCB 101
PCB 118
PCB 105
PCB 153
PCB 138
PCB 128
PCB 187
PCB 180